Final Draft
of the original manuscript:

Sun, X.; Tung, W.; Wang , W.; Xu, X.; Zou, J.; Gould, O.; Kratz, K.; Ma, N.; Lendlein, A.:

The effect of stiffness variation of electrospun fiber meshes of multiblock copolymers on the osteogenic differentiation of human mesenchymal stem cells.

In: Clinical Hemorheology and Microcirculation. Vol. 73 (2019) 219 - 228.
First published online by IOS: November 13, 2019

DOI: 10.3233/CH-199206
https://doi.org/10.3233/CH-199206

The Effect of Stiffness Variation of Electrospun Fiber Meshes of Multiblock Copolymers on the Osteogenic Differentiation of Human Mesenchymal Stem Cells

Xianlei Sun [1, 2,#], Wingtai Tung [1,#], Weiwei Wang [1], Xun Xu[1], Jie Zou[1,3], Oliver E. C. Gould[1], Karl Kratz [1], Nan Ma [1, 3,*] and Andreas Lendlein [1, 2, 3,*]

[1]Institute of Biomaterial Science and Berlin-Brandenburg Center for Regenerative Therapies, Helmholtz-Zentrum Geesthacht, 14513 Teltow, Germany.

[2]Institute of Biochemistry and Biology, University of Potsdam, 14476 Potsdam, Germany.

[3]Institute of Chemistry and Biochemistry, Free University of Berlin, 14195 Berlin, Germany

# These authors contributed equally to this work.

* To whom correspondence should be addressed: Prof. Dr. Nan Ma, Prof. Dr. Andreas Lendlein
Email: nan.ma@hzg.de, andreas.lendlein@hzg.de

Abstract:

Electrospinning has attracted significant attention as a method to produce cell culture substrates whose fibrous structure mimics the native extracellular matrix (ECM). In this study, the influence of E-modulus of fibrous substrates on the lineage commitment of human adipose-derived stem cells (hADSCs) was studied using fiber meshes prepared via the electrospinning of a polyetheresterurethane (PEEU) consisting of poly(ρ-dioxanone) (PPDO) and poly(ε-caprolactone) (PCL) segments. The PPDO:PCL weight ratio was varied from 40:60 to 70:30 to adjust the physiochemical properties of the PEEU fibers. The cells attached on stiffer PEEU70 (PPDO:PCL = 70:30) fiber meshes displayed an elongated morphology compared to those cultured on softer fibers. The nuclear aspect ratio (width vs. length of a nucleus) of hADSCs cultured on softer PEEU40 (PPDO:PCL = 40:60) fibers was lower than on stiffer fibers. The osteogenic differentiation of hADSCs was enhanced by culturing on stiffer fibers. Compared to PEEU40, a 73% increase of osteocalcin expression and a 34% enhancement of alkaline phosphatase (ALP) activity were observed in cells on PEEU70. These results

demonstrated that the differentiation commitment of stem cells could be regulated via tailoring the mechanical properties of electrospun fibers.

Key words: electrospun fibers, polyetheresterurethane, E-modulus, mesenchymal stem cells, osteogenic differentiation

1. Introduction

Mesenchymal stem cells (MSCs), a cell source for bone regeneration [1-3], were originally identified in bone marrow, but can also be obtained from other mesenchymal tissues, avoiding invasive aspirate procedures [4]. Among all sources, adipose tissue is an attractive source for MSC due to its abundance and relative accessibility by using routine liposuction procedures with minimal morbidity [5-7]. MSC differentiation into multiple cell types, including osteoblasts, can be regulated by ECM stiffness in its local microenvironment [8, 9].

Recently, human adipose-derived stem cells (hADSCs) have been widely applied for bone regeneration as a result of their great potential for maintaining the integrity of bone [10-12]. However, large-scale production of clinical-grade hADSC and hADSCs derived osteocyte remains a bottleneck to meet clinical demand due to expense, limited scalability and high batch-to-batch variability of the substrate. Therefore, it is necessary to develop inexpensive, robust, scalable substrates with well-defined biomaterials [13, 14].

Electrospinning is a versatile and efficient technique for the production of nano- and micro-fiber based scaffolds with an inherent porous structure [15]. This technique allows the adjustment of the scaffold morphology, the surface area to volume ratio, and porosity [16]. Further, electrospun fibers can potentially mimic parts of the native extracellular matrix (ECM) in human tissue and provide relevant signals to modulate cells behavior. Electrospun nanofibers can facilitate MSCs' cell attachment and proliferation, and modulate MSCs' differentiation [17].

Poly (ε-caprolactone) (PCL) is a chemically established implantable biomaterial capable of supporting the MSCs' proliferation and osteogenic differentiation *in vitro* [18, 19]. Poly(ρ-dioxanone) (PPDO) is a hydrolytically degradable material and can promote hydrophillity, enhancing cell-material attachment [20]. In this study, a polyetheresterurethane (PEEU) containing poly(ρ-dioxanone) (PPDO) and poly(ε-caprolactone) segments was electrospun into fiber meshes. The effect of substrate stiffness on hADSC behavior was investigated by culturing hADSCs on electrospun PEEU fiber meshes. The cell morphology was carefully studied in terms of the influence of the mechanical properties of the mesh on hADSCs osteogenic differentiation.

2. Materials and Methods

2.1. PEEU synthesis and electrospinning

Polyesteretherurethane (PEEU) polymers with different PPDO to PCL weight ratios (40:60, 50:50, 60:40, 70:30) were synthesized following the procedure described in our previous work [21], named PEEU40, PEEU50, PEEU60 and PEEU70 respectively. L-lysine diisocyanate was used as the linker for poly(ρ-dioxanone) diol and poly(ε-caprolactone) diol.

The fiber meshes were prepared by electrospinning of PEEU. PEEU was dissolved in hexafluoroisopropanol (HFIP) at a concentration of 11 wt% and filtered using a glass fiber filter with 1 µm pore size. The solution was electrospun in a chamber with 20% humidity at the solution flowrate of 2.1 mL/h. The applied voltage ranged from 10 at the beginning to 18 kV at the end of spinning. The fibers were collected on a polypropylene film wrapped drum collector rotating at a speed of 5 rpm, with the distance between the tip to the collector set at 25 cm. Prior to cell culture, the fiber meshes were sterilized using 10% (v/v) ethylene oxide, at 45 ºC and 1.7 bar for 3 hours. The fiber diameter was examined by analyzing the scanning electron microscopic images of the fiber meshes using Image J software (version 1.44; National Institutes of Health). All of the fiber meshes showed the similar average fiber diameter ranging from 1.4 to 1.7 µm.

2.2. Mechanical testing

Test specimens were investigated at ambient temperature with a Zwick Z005 (Zwick GmbH, Ulm, Germany). The stretching rate was kept constant at 10 $mm \cdot min^{-1}$ for all tensile tests. Three to five samples were investigated for each fibrous mesh. The Young's moduli (E) of the fibrous meshes were determined from the stress-strain curve at the strain region of 1% to 5%. The young's modulus of each prepared fiber mesh was measured as 2.6 ± 0.8 MPa (PEEU40), 3.2 ± 0.9 MPa (PEEU50), 4.0 ± 0.9 MPa (PEEU60) and 4.5 ± 0.8 MPa (PEEU70), respectively.

2.3. Cultivation of hADSCs

The hADSCs were isolated from human adipose tissue of a female donor after informed consent (No.: EA2/127/07; Ethics Committee of the Charité - Universitätsmedizin Berlin, approval from 17.10.2008), as described previously [22]. The cells were maintained in human adipose-derived stem cell medium (ADSC^{TM} growth medium, Lonza, Walkersville, MD, USA) at 37 °C in a humid atmosphere containing 5% (v/v) CO_2. The growth medium was changed

every 2 days. The cells were dissociated using 0.25% (w/v) trypsin–EDTA solution when reaching around 90% confluence, and were subcultured to new flasks.

2.4. Cell staining, morphology and nuclear aspect ratio

The cells were seeded on PEEU fiber meshes at the density of 5.0×10^4 / cm^2. After 7 days of incubation in growth medium, the hADSCs were fixed with 4% (w/v) paraformaldehyde (Thermo Fisher Scientific, Waltham, USA), followed by PBS washing for 3 times, with 5 minutes for each. The hADSCs were then permeabilized with 0.02% of triton x-100 in PBS for 10 minutes and washed with PBS for 3 times. Then, 5% (w/v) bovine serum albumin (BSA) in PBS was applied for 1 hour to block non-specific antigens. The cytoskeleton and nuclei were stained with ActinRed™ 555 (Life Technologies, Darmstadt, Germany), and Hoechst 33342 (Life Technologies, Darmstadt, Germany) according to the given protocol. The stained samples were washed with PBS and observed under a confocal laser scanning microscope (LSM 780, Carl Zeiss, Jena, Germany). The aspect ratio of cells and nuclei, and the nuclei size were analyzed using Image J software (National Institutes of Health, USA).

2.5. Differentiation assay

The hADSCs were seeded on the fiber meshes at a density of 1×10^5 cells / cm^2. After 3 days of culture in growth medium to obtain a high cell density, the PEEU fiber meshes were transferred into a new 24-well plate and cultured with the competitive differentiation medium, which was prepared by mixing adipogenesis medium (StemPro® Adipogenesis Differentiation Kit, Thermo Fisher) and osteogenesis medium (StemPro® Osteogenesis Differentiation Kit, Thermo Fisher) at a ratio of 1: 1 (v/v). The competitive differentiation medium was changed every three days. After 3 weeks of culture, the osteogenic differentiation of hADSCs was examined.

2.6. Enzyme-linked immunosorbent assay (ELISA)

The osteogenic differentiation of hADSCs on different PEEU fiber meshes was studied by quantification of osteocalcin (OCN) using ELISA. The hADSCs cultured in the competitive

differentiation medium for 3 weeks were lysed using the RIPA Lysis and Extraction Buffer (Thermo Fisher Scientific, Waltham, Massachusetts, USA) containing a mixture of 1× Halt Protease and Phosphatase Inhibitor Cocktail (Thermo Fisher Scientific, Waltham, Massachusetts, USA). The lysate was centrifuged with a centrifugal force of 15000 g for 15 min and the protein concentration in the supernatant was measured using a BCA protein assay kit (Thermo Fisher Scientific, Bonn, Germany). The osteocalcin in the supernatant was quantified using the Human Osteocalcin-ELISA kit (Invitrogen, California, USA), and was normalized by the amount of total protein in the extract which measured using a BCA protein assay kit (Thermo Fisher Scientific, Bonn, Germany).

2.7. ALP activity quantification

The hADSCs were cultured on different PEEU fiber meshes in the competitive differentiation medium for 3 weeks. The cells were lysed, and the supernatant was collected for measuring ALP activity using an alkaline phosphatase assay kit (Abcam, Berlin, Germany). The results were normalized by the amount of total protein.

2.8. Mineralization assay

After 3 weeks of culture in mixed differentiation media, the cells were fixed with 4% (w/v) paraformaldehyde (ThermoFisher Scientific, Waltham, USA) for 20 minutes. The OsteoImage™ Mineralization Assay kit (Lonza, Walkersville, MD, USA) was used to stain the hydroxyapatite. The cell nucleus was stained with Hoechst 33342 (Life Technologies, Darmstadt, Germany). The stained samples were then imaged using a confocal laser scanning microscope (LSM 780, Carl Zeiss, Jena, Germany). The fluorescence intensity of the stained hydroxyapatite was analyzed using Image J software (National Institutes of Health, USA).

2.9. Statistics

The number of replications for experiments was indicated in the figure legends for each assay. The data are presented as mean ± standard deviation. Statistical analysis was performed using the two-tailed independent-samples t test, and a p value less than 0.05 was considered as statistically significant.

3. Results and discussion

3.1 hADSC morphology on PEEU fiber meshes

In this study, the effect of the stiffness of PEEU fiber meshes on the morphology of hADSCs was investigated. The cells attached on all of the PEEU fibers exhibited a variation in cell morphology (Fig. 1a). After 7 days of culture in a growth medium, the cells on stiffer fiber meshes (PEEU60 and PEEU70) were highly elongated compared to the cells on softer fiber meshes (PEEU40 and PEEU50) (Fig. 1b). Stronger and highly aligned F-actin stress fibers could be observed in cells on PEEU70 (Fig. 1a). It is known that MSCs display a more widely spread morphology on stiffer surfaces than on their softer counterparts. The stiffer surface potentially facilitates the formation and organization of F-actin cytoskeleton [23]. In agreement with work reported elsewhere, our results indicated that the morphology of hADSCs was highly related to the E-modulus of the PEEU fiber meshes.

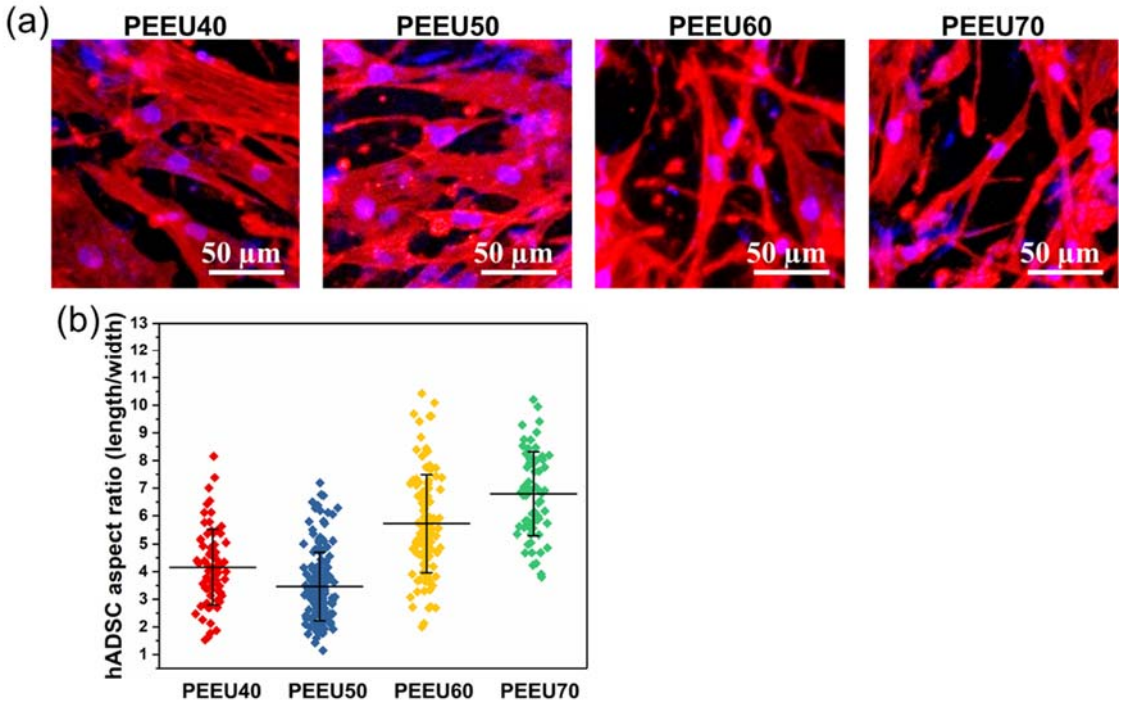

Figure 1. The stiffness of PEEU fibers modulates the morphology of hADSCs. (a) Representative images of cells cultured on different fiber meshes in growth medium for 7 days. Cells were stained to visualize the F-actin cytoskeleton (red) and nuclei (blue) (scale bar = 20 µm). (b) The aspect ratio of hADSCs on PEEU fiber meshes. The number of cells counted for analysis was: $n_{PEEU40} = 381$; $n_{PEEU50} = 383$; $n_{PEEU60} = 376$; $n_{PEEU70} = 425$ (*$p < 0.05$).

3.2 Nuclear shape of hADSCs on PEEU fiber meshes

Cell nuclei are able to perceive mechanical stimuli from culture substrates through the cytoskeleton. Although intracellular tension can be partially balanced by the nucleus, higher tension induces the shape change of cell nucleus. For example, nuclear shape change has been demonstrated to be induced by the rigidity of cell culture substrate [24-27]. Changes in nuclear shape could explain conformational changes in chromatin structure and organization, which directly regulate the transcription process and consequently modulate stem cell growth or differentiation [28]. Based on the observed shape change of hADSCs on PEEU fiber meshes with different stiffness's, the fiber meshes were expected to have an effect on the nuclear shape of hADSCs.

After 7 days of culture on the fiber meshes, the cells were stained with Hoechst 33342 to analyze their nuclear shape. The round shaped nuclei could be observed in the cells on softer fiber meshes (PEEU40 and PEEU50), while the relatively elongated nuclei were found in cells on stiffer fiber meshes (PEEU60 and PEEU70) (Fig. 2a).

Analysis of nuclear aspect ratio and size illustrated that the cells on PEEU40 exhibited the lowest aspect ratio of cell nuclei. The nuclei were elongated with the increase of fiber mesh stiffness. The aspect ratio of cell nuclei on PEEU50, PEEU60 and PEEU70 was significantly higher than on PEEU40 (Fig. 2b). In addition, the cells on PEEU40 had the significantly larger nuclei ($193.7 \pm 70.9\ \mu m^2$) than the cells on other fiber meshes (PEEU50: $147.4 \pm 44.9\ \mu m^2$; PEEU60: $163.3 \pm 48.0\ \mu m^2$; PEEU70: $185.7 \pm 60.9\ \mu m^2$) (Fig. 2b). These results suggested that the stiffness of PEEU fiber meshes could effectively influence the cell shape and morphology. The mechanical force could be transmitted from the cell-fiber interface to the cell

nuclei, potentially regulating cell behavior such as differentiation.

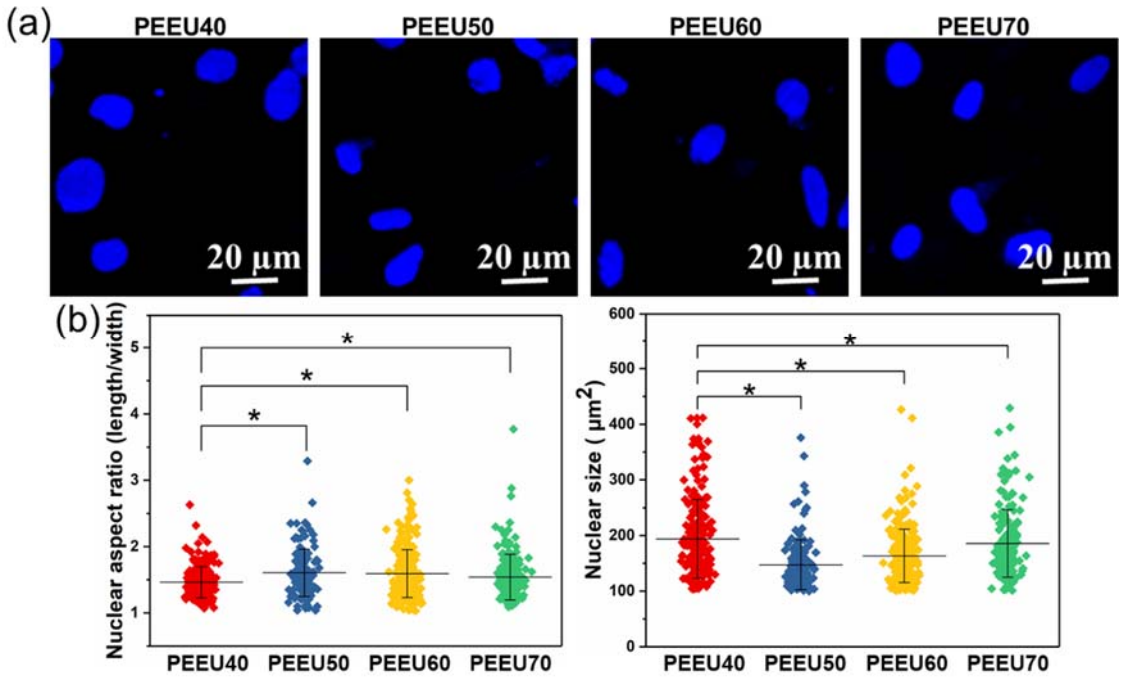

Figure 2. The stiffness of PEEU fibers influences the nuclear shape of hADSCs. (a) Representative images of nuclei (blue) of hADSCs cultured on different fiber meshes in growth medium for 7 days. The nuclei were stained with Hoechst 33342 (scale bar = 20 μm). (b) The nuclear aspect ratio (left) and size (right) of hADSCs cultured on different PEEU fiber meshes for 7 days. The number of cell nuclei counted for analysis was: $n_{PEEU40} = 215$; $n_{PEEU50} = 311$; $n_{PEEU60} = 258$; $n_{PEEU70} = 172$ (*$p < 0.05$).

3.3 ADSCs density on fiber meshes scaffolds

Cell density plays a vital role in regulating mesenchymal stem cell differentiation [29, 30]. The differentiation of hMSCs started with low cell density promotes osteogenic differentiation while high cell density promotes adipogenic differentiation [31]. Therefore, in order to study the effect of fiber mesh stiffness on osteogenic differentiation of hADSCs, the influence of cell density should be eliminated. To regulate the cell density of the hADSCs at the beginning of differentiation, the cell were seeded on the meshes with a high cell number (1×10^5 cells / cm^2). After 3 days of culture in growth medium, the cell density on the fiber meshes was evaluated via staining the F-actin and cell nuclei (Fig. 3a). The cells on different fiber meshes had the similar cell density (Fig. 3b), suggesting the similar cell attachment of hADSCs on the PEEU

fiber meshes. The differentiation experiment could then be performed with a similar cell density from the beginning of the process.

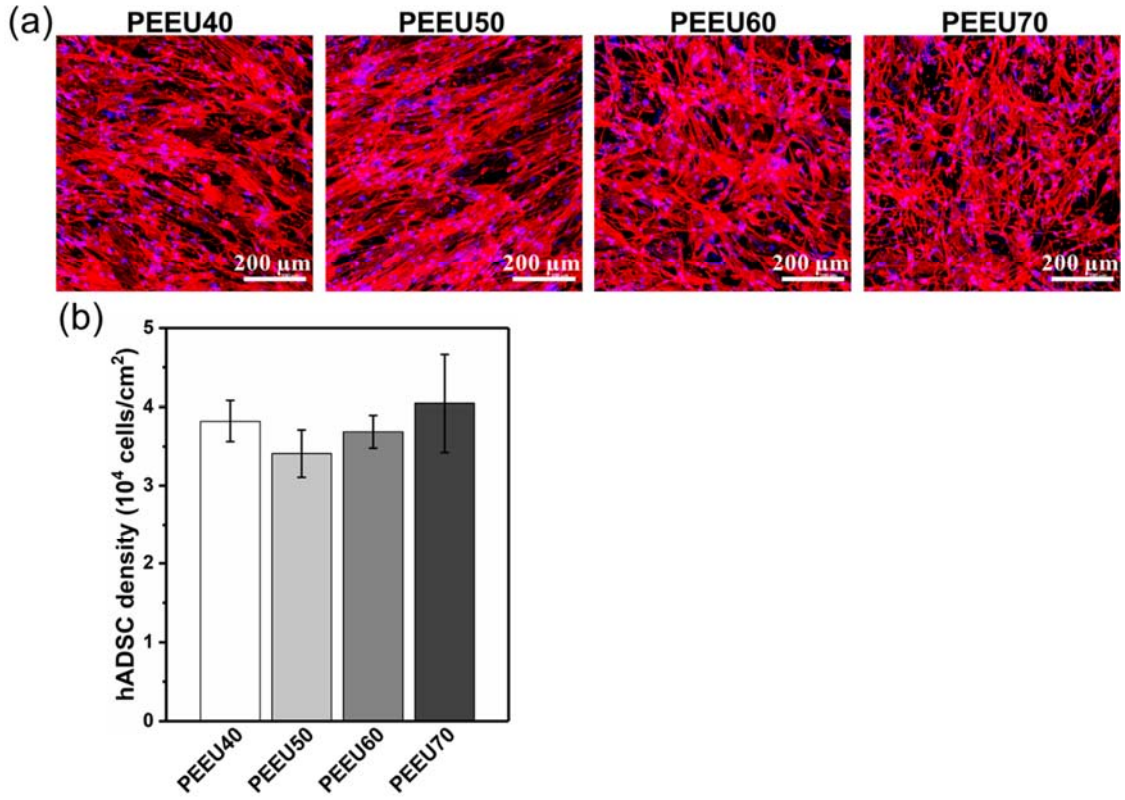

Figure 3. The density of hADSCs on fiber meshes scaffolds. Cells were seeded with a high density, and were stained to visualize F-actin cytoskeleton (red) and nuclei (blue) after 3 days of culture in growth medium. (a) Representative images of hADSCs on different fiber meshes (scale bar = 200 μm). (b) The density of hADSCs assessed by counting the cell nuclei in the fluorescent images. The number of the images for analysis was: $n_{PEEU40} = 4$; $n_{PEEU50} = 3$; $n_{PEEU60} = 4$; $n_{PEEU70} = 4$.

3.4 Osteogenic differentiation of hADSCs on PEEU fiber meshes

The expression of osteogenic marker – osteocalcin in hADSCs cultured on PEEU fiber meshes for 3 weeks in competitive differentiation medium was quantified using an ELISA kit. An increasing trend of osteocalcin level was observed with the increase of fiber mesh stiffness (Fig. 4a). The osteocalcin level in cells on stiffer fiber meshes (PEEU50, PEEU60 and PEEU70) was significantly higher than that on the softer PEEU40 fiber mesh. The activity of bone-specific alkaline phosphatase (ALP) was examined to evaluate the osteogenic differentiation

of hADSCs on the fiber meshes. The highest ALP activity was found in the cells cultured on PEEU70 fiber mesh, which was significantly higher than that in other groups (Fig. 4b). These results suggested that the fiber mesh with a higher E-modulus could effectively enhance osteogenesis of hADSCs compared to the softer fiber meshes.

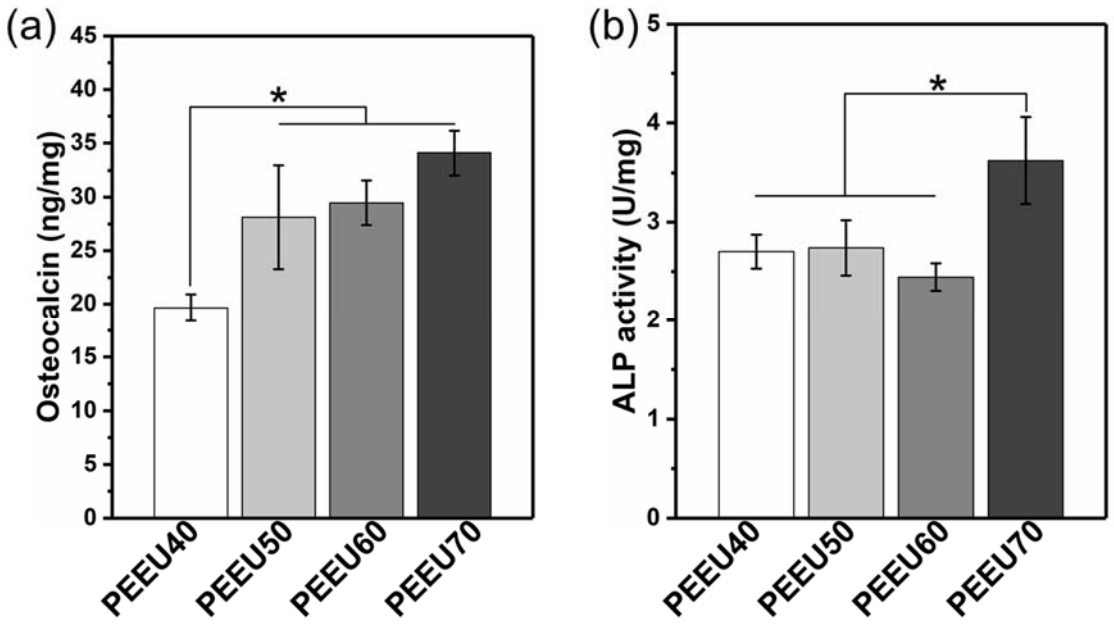

Figure 4. PEEU fiber with a higher stiffness enhances the osteogenic differentiation of hADSCs. The cells were cultured in competitive differentiation medium for 3 weeks. (a) The osteocalcin expression of hADSCs on different fiber meshes was normalized by the amount of total protein ($n_{PEEU40} = 6$; $n_{PEEU50} = 6$; $n_{PEEU60} = 6$; $n_{PEEU70} = 6$). (b) The ALP activity of hADSCs on different fiber meshes was normalized by the total amount of protein. ($n_{PEEU40} = 5$; $n_{PEEU50} = 5$; $n_{PEEU60} = 4$; $n_{PEEU70} = 6$). ($*p < 0.05$)

3.5 Fluorescence imaging of osteoblast mineralization

Cells remodel their surrounding ECM by producing extracellular matrix proteins and regulators of matrix mineralization during osteogenic differentiation. Mature osteoblasts are typically indicated with mineralized matrix as they deposit hydroxyapatite crystals [32]. To examine the osteogenic differentiation of hADSCs on the fiber meshes, the samples were stained to evaluate the abundance of hydroxyapatite (Fig. 5a). A higher level of hydroxyapatite was detected on stiffer fiber meshes (Fig. 5b left). The quantification data normalized by cells number showed that the hydroxyapatite amount gradually increased with the increase of fiber mesh E-modulus

(Fig. 5b right), with the highest fluorescence intensity of hydroxyapatite found on PEEU70 fiber mesh. The results confirmed the enhancement of osteogenic differentiation of hADSCs in the materials with higher fiber mesh stiffness.

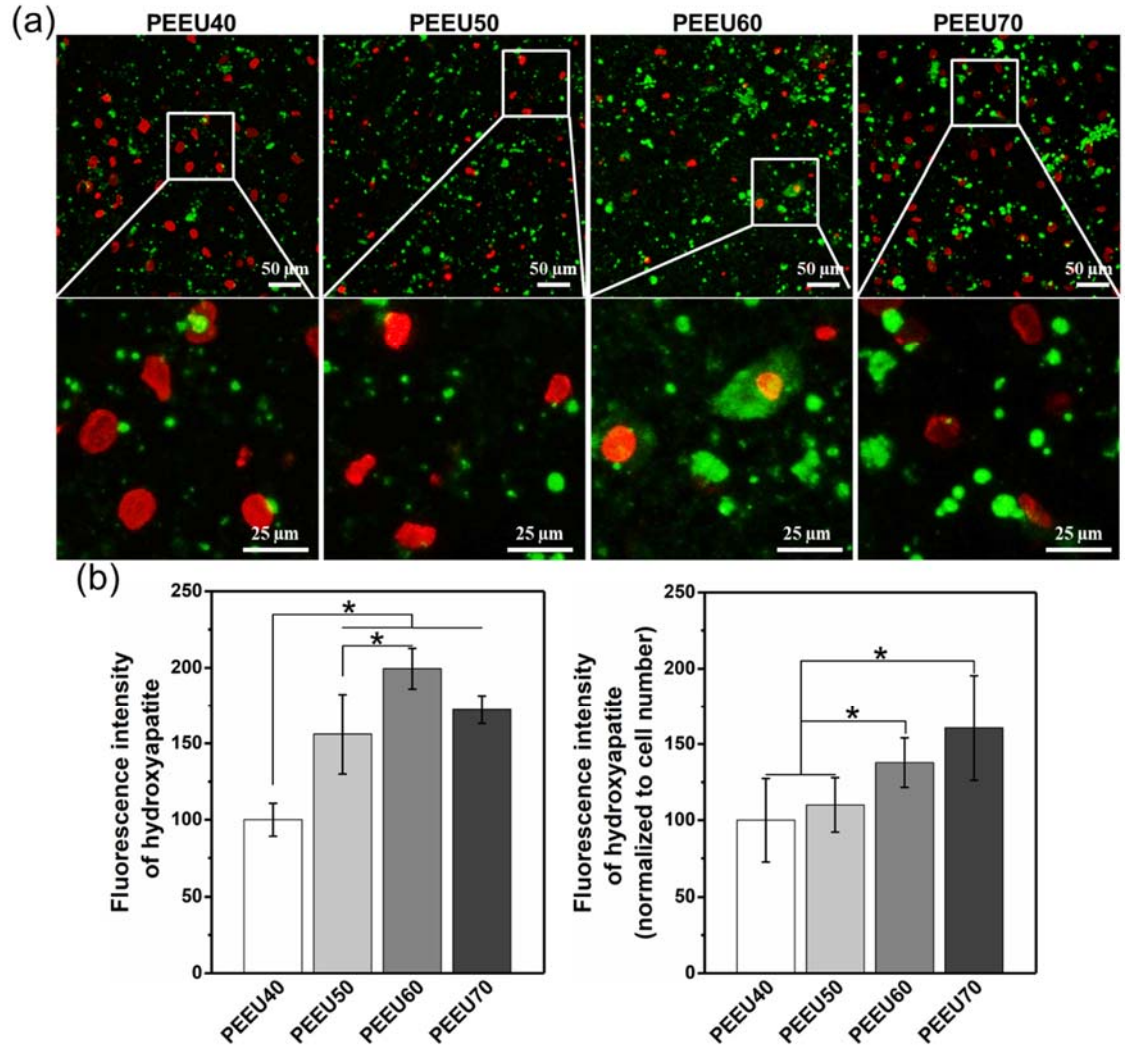

Figure 5. PEEU fiber meshes with higher stiffness enhance the mineralization of hADSCs. The cells were cultured in a competitive differentiation medium for 3 weeks. (a) Representative images of hADSCs on different fiber meshes. The cells were stained to visualize the nuclei (red) and deposited hydroxyapatite (green) (scale bar = 50 μm in upper panel and 25 μm in lower panel). (b) The fluorescent intensity of stained hydroxyapatite on different fiber meshes, without (left) and with (right) normalization by cell number. The cell number was determined by counting the cell nuclei in the images. The number of images used for analysis was: $n_{PEEU40} = 7$; $n_{PEEU50} = 8$; $n_{PEEU60} = 11$; $n_{PEEU70} = 10$. (*$p < 0.05$)

4. Conclusion

In this study, the mechanical properties of PEEU fiber meshes prepared via electrospinning could be tailored by varying the PPDO:PCL weight ratio. The increase of PPDO ratio in the multiblock copolymer resulted in an increase of the E-modulus of the fiber mesh. Compared to hADSCs cultured on softer fiber meshes (e.g. PEEU40), the hADSCs cultured on the stiffer fiber meshes (e.g. PEEU70) exhibited elongated cell shape as well as the higher nuclear aspect ratio. The increase of the E-modulus of the fiber mesh significantly enhanced the osteogenic differentiation of hADSCs, providing insight in the fabrication of function-oriented biomimetic fibrous scaffolds to improve bone regeneration.

Acknowledgements

This work was financially supported by the Helmholtz Association of German Research Centers through program-orientated funding and through Helmholtz Graduate School for Macromolecular Bioscience (MacroBio), grant no. VH-GS-503 (X. S., W. T., and J. Z. X. S. gratefully acknowledges the financial support of the China Scholarship Council (CSC), grant no. 201506010267.

References

1. Jin, Y.-Z. and J.H. Lee, *Mesenchymal Stem Cell Therapy for Bone Regeneration.* Clinics in orthopedic surgery, 2018. **10**(3): p. 271-278.
2. Zomorodian, E. and M. Baghaban Eslaminejad, *Mesenchymal Stem Cells as a Potent Cell Source for Bone Regeneration.* Stem Cells International, 2012. **2012**: p. 9.
3. Grayson, W.L., et al., *Stromal cells and stem cells in clinical bone regeneration.* Nature Reviews Endocrinology, 2015. **11**: p. 140.
4. James, A.W., *Review of Signaling Pathways Governing MSC Osteogenic and Adipogenic Differentiation.* Scientifica (Cairo), 2013. **2013**: p. 684736.
5. James, A.W., et al., *Perivascular stem cells: a prospectively purified mesenchymal stem cell population for bone tissue engineering.* Stem Cells Transl Med, 2012. **1**(6): p. 510-9.
6. Mizuno, H., M. Tobita, and A.C. Uysal, *Concise review: Adipose-derived stem cells as a novel tool for future regenerative medicine.* Stem Cells, 2012. **30**(5): p. 804-10.
7. Levi, B. and M.T. Longaker, *Concise review: adipose-derived stromal cells for skeletal regenerative medicine.* Stem Cells, 2011. **29**(4): p. 576-82.
8. Chamberlain, G., et al., *Concise review: mesenchymal stem cells: their phenotype, differentiation capacity, immunological features, and potential for homing.* Stem Cells, 2007. **25**(11): p. 2739-49.

9. Sun, M., et al., *Extracellular matrix stiffness controls osteogenic differentiation of mesenchymal stem cells mediated by integrin α5.* Stem cell research & therapy, 2018. **9**(1): p. 52-52.
10. Levi, B. and M.T. Longaker, *Concise Review: Adipose-Derived Stromal Cells for Skeletal Regenerative Medicine.* STEM CELLS, 2011. **29**(4): p. 576-582.
11. Brett, E., et al., *Human Adipose-Derived Stromal Cell Isolation Methods and Use in Osteogenic and Adipogenic In Vivo Applications.* Current protocols in stem cell biology, 2017. **43**: p. 2H.1.1-2H.1.15.
12. Grottkau, B.E. and Y. Lin, *Osteogenesis of Adipose-Derived Stem Cells.* Bone Research, 2013. **1**: p. 133.
13. O'Brien, F.J., *Biomaterials & scaffolds for tissue engineering.* Materials Today, 2011. **14**(3): p. 88-95.
14. Bružauskaitė, I., et al., *Scaffolds and cells for tissue regeneration: different scaffold pore sizes-different cell effects.* Cytotechnology, 2016. **68**(3): p. 355-369.
15. Deitzel, J.M., et al., *Controlled deposition of electrospun poly(ethylene oxide) fibers.* Polymer, 2001. **42**(19): p. 8163-8170.
16. Li, D. and Y. Xia, *Electrospinning of Nanofibers: Reinventing the Wheel?* Advanced Materials, 2004. **16**(14): p. 1151-1170.
17. Min, B.M., et al., *Electrospinning of silk fibroin nanofibers and its effect on the adhesion and spreading of normal human keratinocytes and fibroblasts in vitro.* Biomaterials, 2004. **25**(7-8): p. 1289-97.
18. Yoshimoto, H., et al., *A biodegradable nanofiber scaffold by electrospinning and its potential for bone tissue engineering.* Biomaterials, 2003. **24**(12): p. 2077-82.
19. Porter, J.R., A. Henson, and K.C. Popat, *Biodegradable poly(epsilon-caprolactone) nanowires for bone tissue engineering applications.* Biomaterials, 2009. **30**(5): p. 780-8.
20. Wang, H., et al., *Synthesis of PDON-b-PEG-b-PDON block copolymers and drug delivery system thereof.* Journal of Applied Polymer Science, 1998. **68**(13): p. 2121-2128.
21. Kratz, K., et al., *Shape-Memory Properties and Degradation Behavior of Multifunctional Electro-Spun Scaffolds.* The International Journal of Artificial Organs, 2011. **34**(2): p. 225-230.
22. Xu, X., et al., *Controlling major cellular processes of human mesenchymal stem cells using microwell structures.* Adv Healthc Mater, 2014. **3**(12): p. 1991-2003.
23. Olivares-Navarrete, R., et al., *Substrate Stiffness Controls Osteoblastic and Chondrocytic Differentiation of Mesenchymal Stem Cells without Exogenous Stimuli.* PLoS One, 2017. **12**(1): p. e0170312.
24. Chancellor, T.J., et al., *Actomyosin tension exerted on the nucleus through nesprin-1 connections influences endothelial cell adhesion, migration, and cyclic strain-induced reorientation.* Biophys J, 2010. **99**(1): p. 115-23.
25. Lombardi, M.L., et al., *The interaction between nesprins and sun proteins at the nuclear envelope is critical for force transmission between the nucleus and cytoskeleton.* J Biol Chem, 2011. **286**(30): p. 26743-53.
26. Maniotis, A.J., C.S. Chen, and D.E. Ingber, *Demonstration of mechanical connections between integrins, cytoskeletal filaments, and nucleoplasm that stabilize nuclear structure.* Proc Natl Acad Sci U S A, 1997. **94**(3): p. 849-54.
27. Lovett, D.B., et al., *Modulation of Nuclear Shape by Substrate Rigidity.* Cell Mol Bioeng, 2013. **6**(2): p. 230-238.
28. Dahl, K.N., A.J. Ribeiro, and J. Lammerding, *Nuclear shape, mechanics, and mechanotransduction.* Circ Res, 2008. **102**(11): p. 1307-18.
29. Bitar, M., et al., *Effect of cell density on osteoblastic differentiation and matrix degradation of biomimetic dense collagen scaffolds.* Biomacromolecules, 2008. **9**(1): p. 129-35.

30. Lu, H., et al., *Effect of cell density on adipogenic differentiation of mesenchymal stem cells.* Biochem Biophys Res Commun, 2009. **381**(3): p. 322-7.
31. McBeath, R., et al., *Cell shape, cytoskeletal tension, and RhoA regulate stem cell lineage commitment.* Dev Cell, 2004. **6**(4): p. 483-95.
32. Jensen, E.D., R. Gopalakrishnan, and J.J. Westendorf, *Regulation of gene expression in osteoblasts.* Biofactors, 2010. **36**(1): p. 25-32.